Supplementary Material

Spinning continuous high-strength bacterial cellulose hydrogel fiber for multifunctional bioelectronic interfaces

Minghao Zhang, Shiyan Chen, Nan Sheng, Baoxiu Wang, Zhuotong Wu, Qianqian Liang, Zhiliang Han, Huaping Wang**

State Key Laboratory for Modification of Chemical Fibers and Polymer Materials, College of Materials Science and Engineering, Donghua University, Shanghai 201620, PR China

Email addresses: chensy@dhu.edu.cn; wanghp@dhu.edu.cn

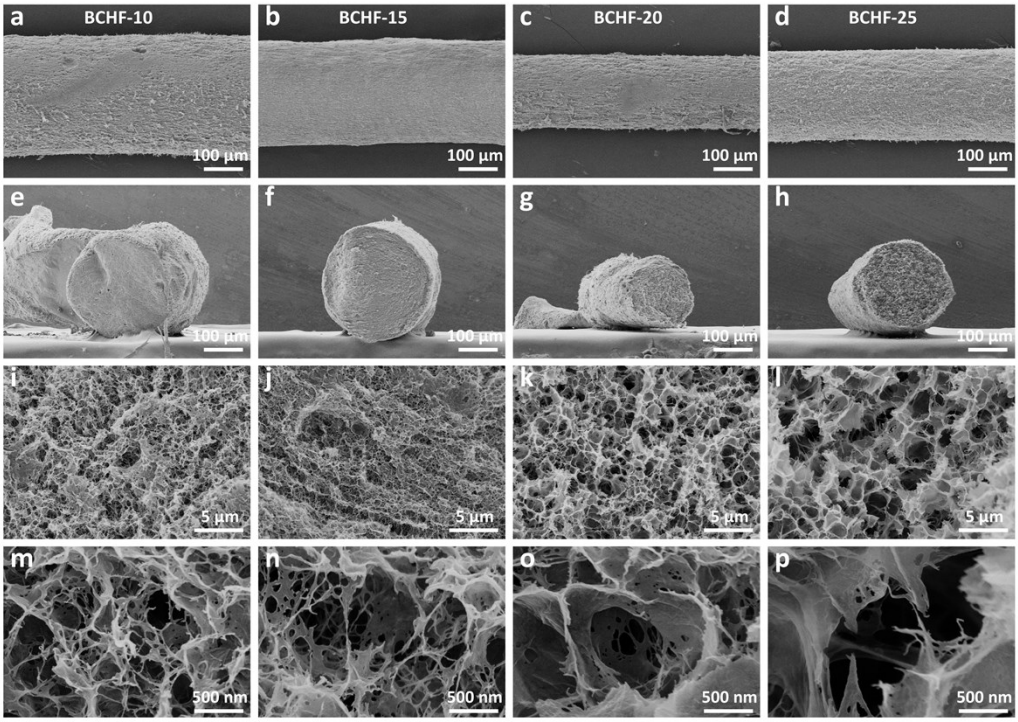

Fig. S1. SEM images of BCHFs with different urea contents of 10 wt%, 15 wt%, 20 wt%, and 25 wt%. **(a-d)** The surface SEM images of BCHFs. **(e-h)** The cross-sectional SEM images of BCHFs. **(i-l), (m-p)** The cross-sectional SEM images of BCHFs with different magnification.

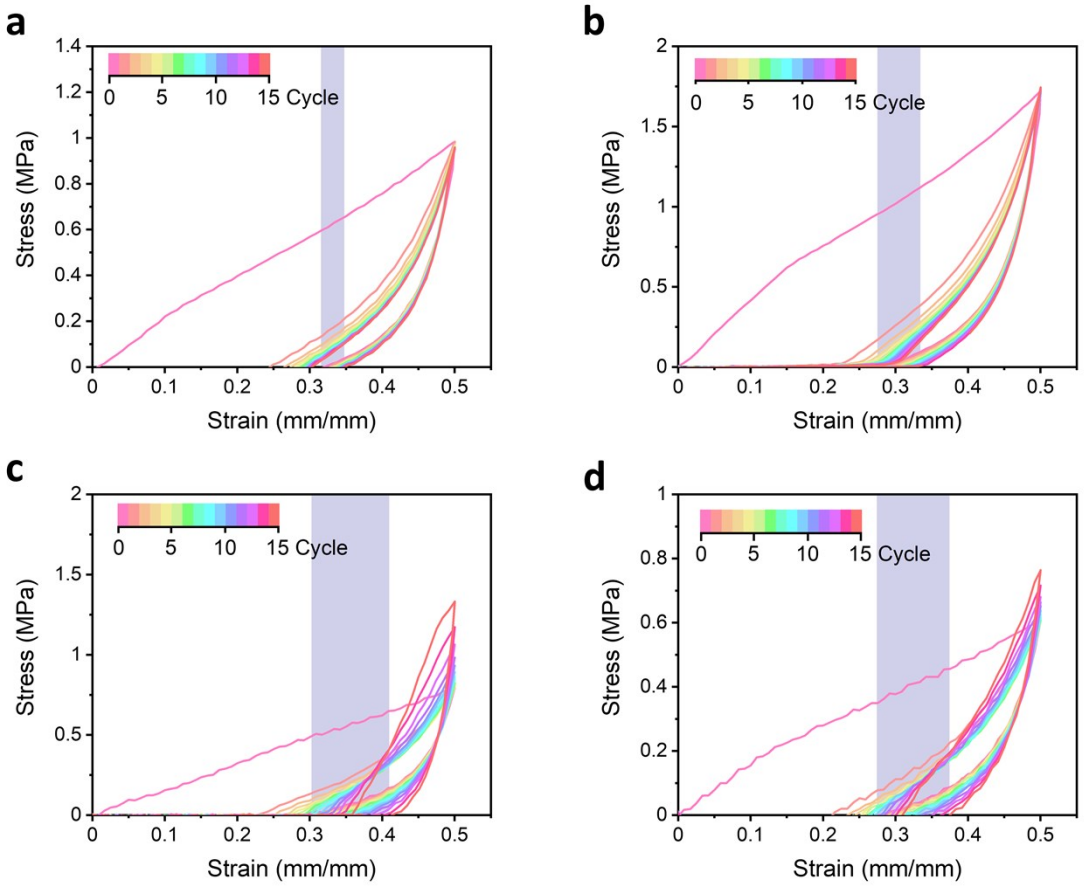

Fig. S2. Representative tensile stress–strain curves of BCHF-10 (a), BCHF-15 (b), BCHF-20 (c) and BCHF-25 (d) during loading–unloading cycles of fixed strains.

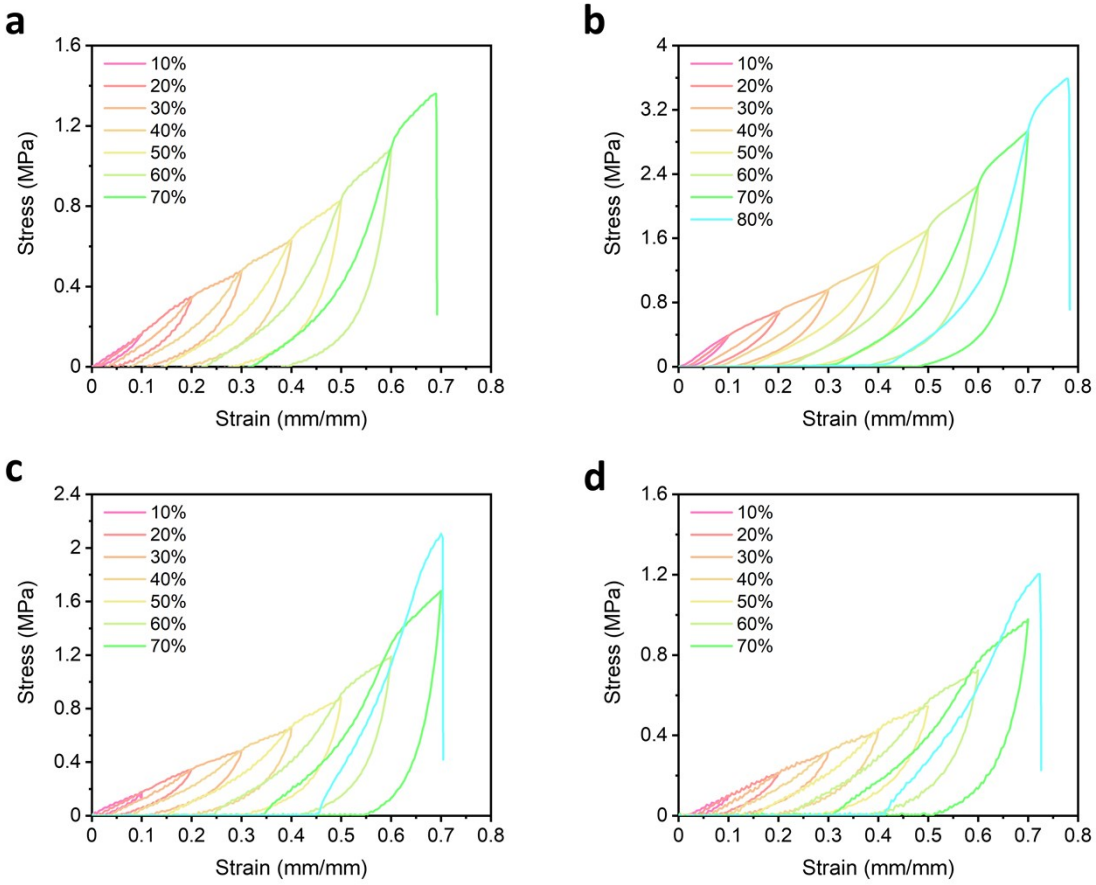

Fig. S3. Representative tensile stress–strain curves of BCHF-10 (a), BCHF-15 (b), BCHF-20 (c) and BCHF-25 (d) during loading–unloading cycles with various strains.

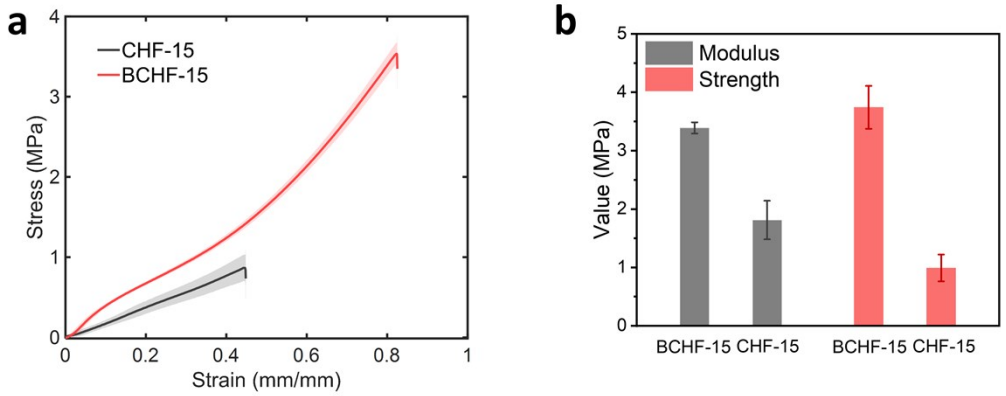

Fig. S4. (a) The tensile stress-strain curves as well as (b) elastic modulus and tensile strength value of BCHF-15 and CHF-15 obtained under the same preparation conditions, showing the irreplaceable role of nanofibers in BCHFs.

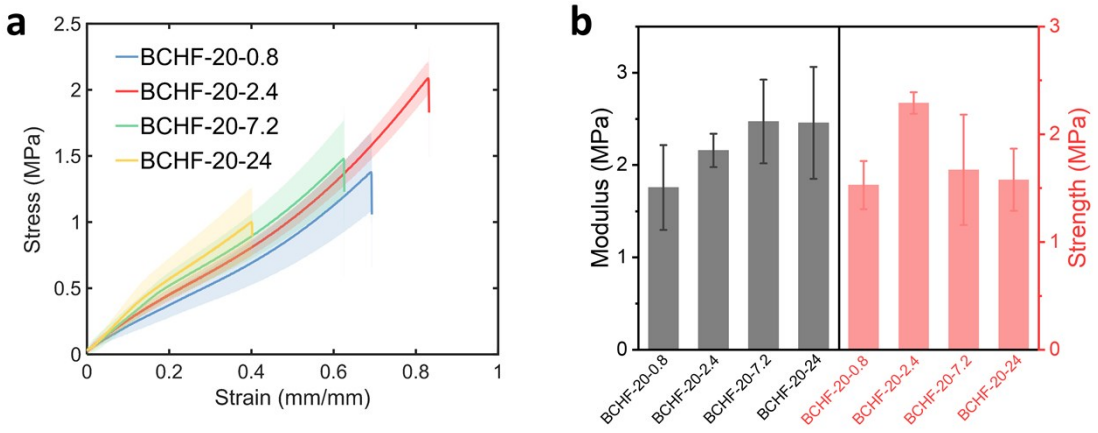

Fig. S5. (a) The tensile stress-strain curves as well as (b) elastic modulus and tensile strength of BCHF-20 with different spin speeds.

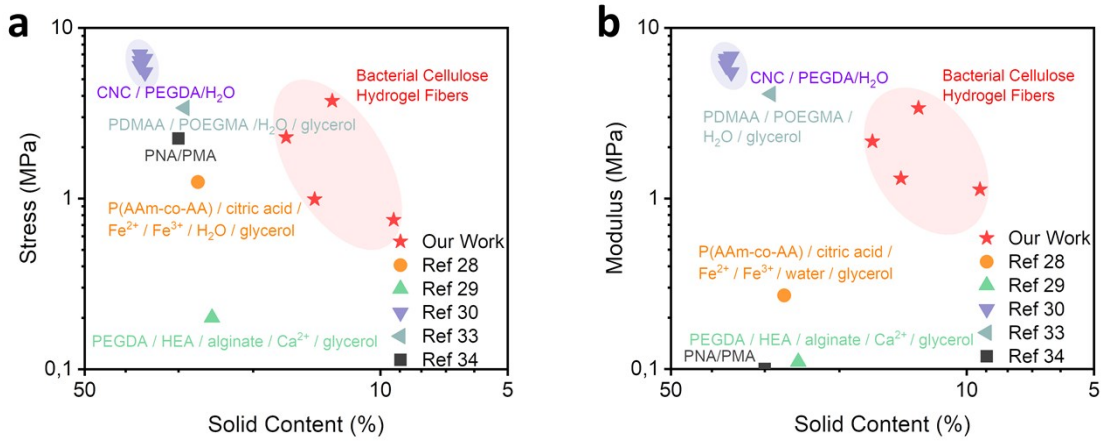

Fig. S6. Stress and modulus to the solid content of BCHFs compared with those of other reported hydrogel fibers and organohydrogel fibers obtained by spinning.

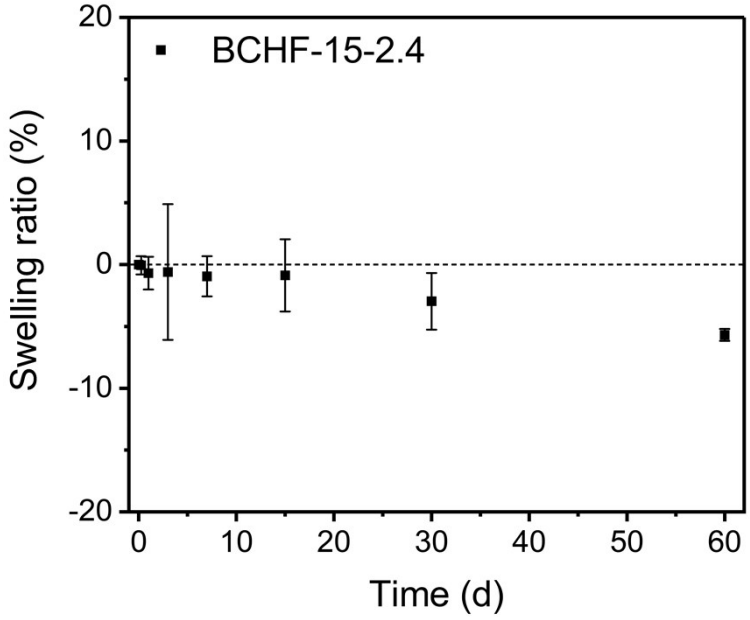

Fig. S7. Swelling ratio (g/g) curve of BCHF-15-2.4. The equilibrium swelling rate of BCHF-15-2.4 does not increase after soaking in water for 60 days. A minor quality loss after a long time in the water may come from the slight degradation.

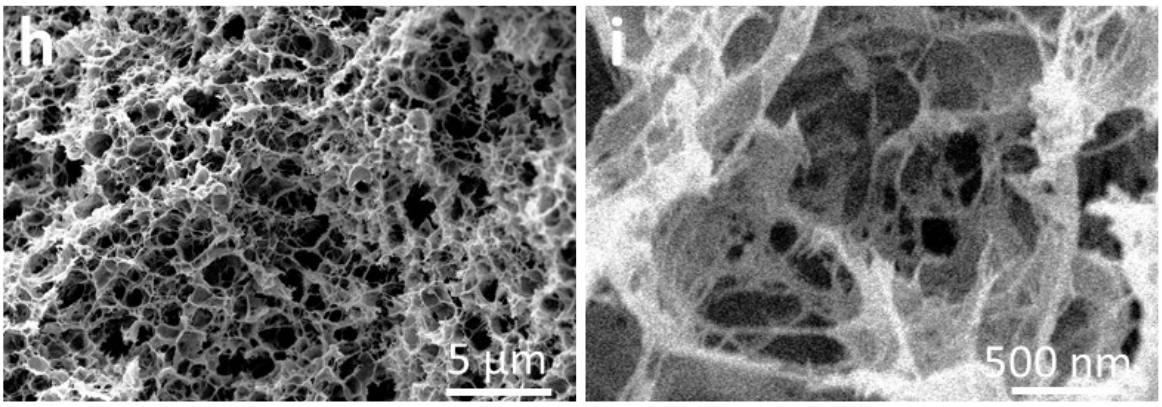

Fig S8. SEM images of BCHF-15-2.4 after being immersed in water for 60 days.

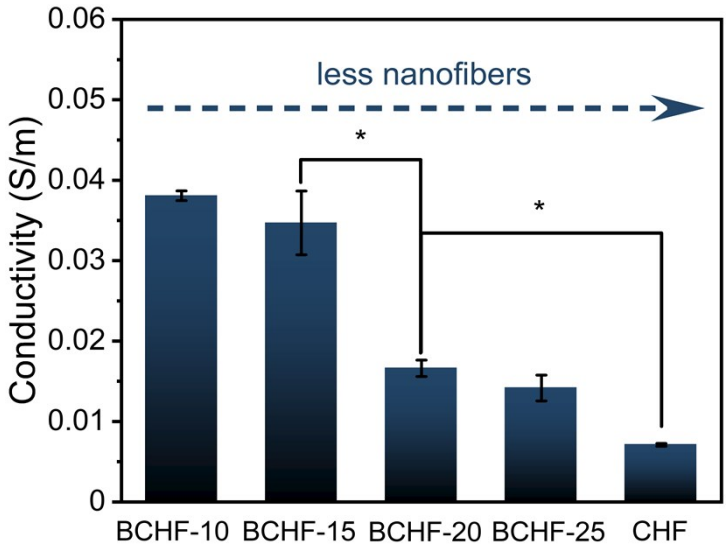

Fig. S9. Ionic conductivity of BCHFs and CHF. The conductivity of hydrogel fibers with more nanofibers is higher, indicating that the presence of nanofibers has a positive effect on the electrical conductivity.

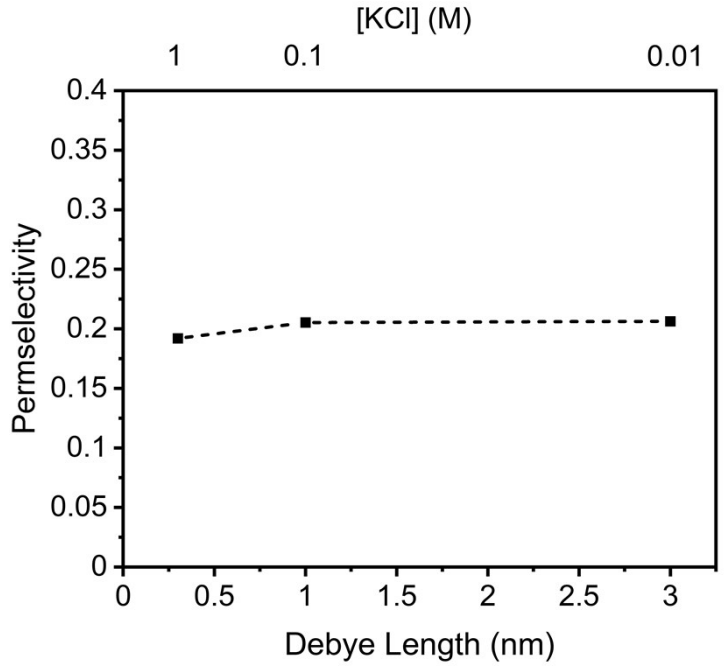

Fig. S10. The measured permselectivity values of BCHF-15 were plotted as a function of the Debye length and KCl concentration.

The ion selectivity can be quantified by measuring the open-circuit voltage according to equation S1,[1] because the static current generated by ion selectivity will cause the generation of voltage (See Materials and Methods for details).

$$t^+ = \frac{1}{2}\left(\frac{E_{diff}}{\frac{RT}{zF}\ln\left(\frac{\gamma_H c_H}{\gamma_L c_L}\right)} + 1\right) \qquad (S1)$$

where t^+ is the cation transference number, which equals 1 for ideal cation selective case and equals 0 for ideal anion selective case. R, T, z, F, γ, c represent the gas constant, temperature, charge valent, Faraday constant, activity coefficient of ions, ion concentrations, respectively.

The permselectivity (P) was then calculated by equation (S2) using the cation transport number in bulk (t^+_{bulk} = 0.49 for KCl solution):

$$P = \frac{t^+ - t^+_{bulk}}{1 - t^+_{bulk}} \qquad (S2)$$

As shown in Fig. S10, the permselectivity of BCHF-15 in each concentration is about +0.21, which indicates the existence of cation selectivity. And it will decrease as the salt concentration increases.

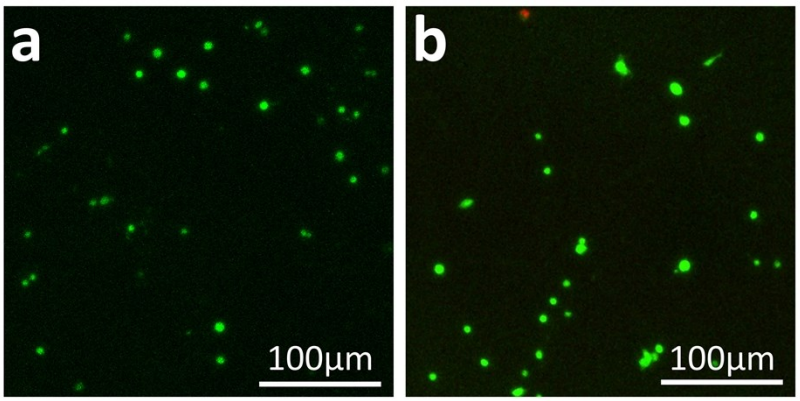

Fig. S11. Laser confocal images of cells on the surface of BCHS (a) and p-BCHS (b) after culturing for 3 days.

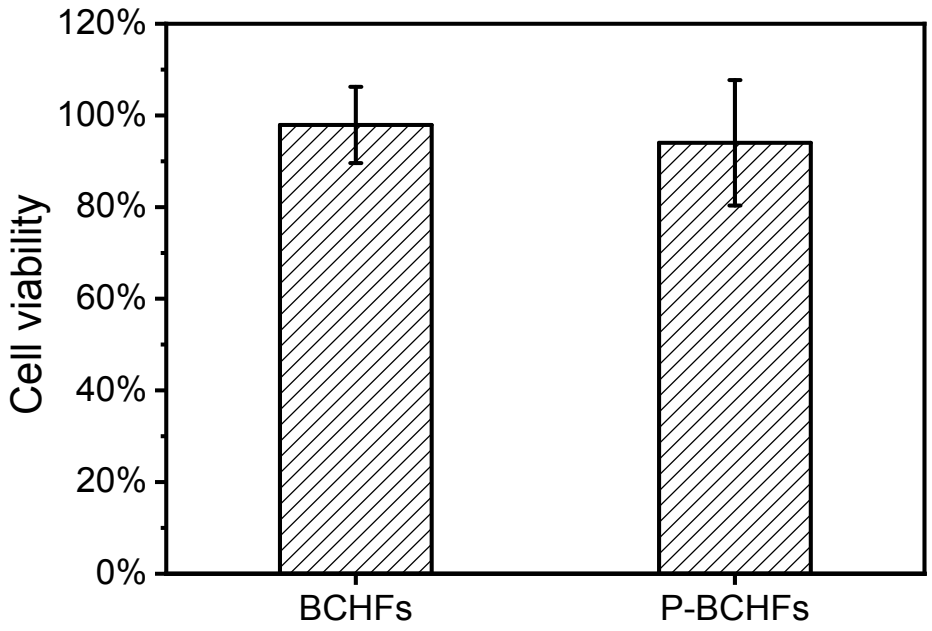

Fig. S12. Cell viability measured by incubating the cells with culture medium that have soaked with BCHFs and p-BCHFs.

Model and theoretical derivation of ionic conductivity of macroscopic nanofluidic devices with channels of various sizes

In our work, the nanofluid space between the micro fibrils in BC nanofibers is considered to be a negatively charged nanochannel with a height of h immersed in the KCl solution, and a constant ion mobility and a constant net surface charge are assumed. The conductance G [S] of a single nanochannel in nanofibers for all KCl concentrations can be described as the superimposition of the bulk conductance and the excess counterion conductance:[2]

$$G = 10^{-3} z(\mu_+ + \mu_-) c N_A e \frac{wh}{d} + 2\sigma_s^* u_+ \frac{w}{d} \qquad (S3)$$

where Z is the cation valence, μ_+ and μ_- [$m^2\ V^{-1}\ s^{-1}$] are the mobility of the cation (K^+) and anion (Cl^-), respectively, c [M=mol L^{-1}] is the concentration of ion, N_A [mol^{-1}] is the Avogadro constant, and e [C] is the electron charge, w [m], h [m] and d [m] are the width, height and length of the nanochannel, σ_s^* [C m^{-2}] is the effective surface charge density.

According to the relationship between conductance and conductivity (equation S4):

$$\sigma = \frac{Gd}{wh} \qquad (S4)$$

The conductivity of a single channel can be expressed as equation S5:

$$\sigma = 10^{-3} z(\mu_+ + \mu_-) c N_A e + \frac{2\mu_+ \sigma_s^*}{h}$$

As shown in Fig. S13, we devoloped a model to subtract the error caused by the area occupied by the entity part of the hydrogel (that is, the part that not allow ions transmission), and the effective conductivity (σ_e) curve of the hydrogel fiber (Fig. S14) can be obtained. In this model, a thin slice of hydrogel fiber cut along the cross section is regarded as composed of the through channel (the length ***d*** of the channel and the length ***L*** of the hydrogel). Then we can deduce euqation S6, S7:

$$s_e = \alpha s_h \ (0 < \alpha < 1) \qquad (S6)$$

$$\sigma_e = \frac{G_e d}{s_e} = \frac{G_h L}{s_e} = \frac{1}{\alpha}\sigma_h \qquad (S7)$$

where S_e is the effective area of ion channels, S_h is the measured cross-sectional area of the hydrogel. σ_e is the effective conductivity of the channels, and its value is more similar to the measured conductivity value of the bulk KCl when the concentration is higher (here we estimated it at KCl concentration of 1 M). σ_h is the measured conductivity of hydrogels. α is the ratio of the effective area to the cross-sectional area of the hydrogel fiber, which can be calculated using equation (S6). Then the effective conductivity σ_e of BCHF-15 at different concentrations can be obtained and plotted in Fig. S13**.**

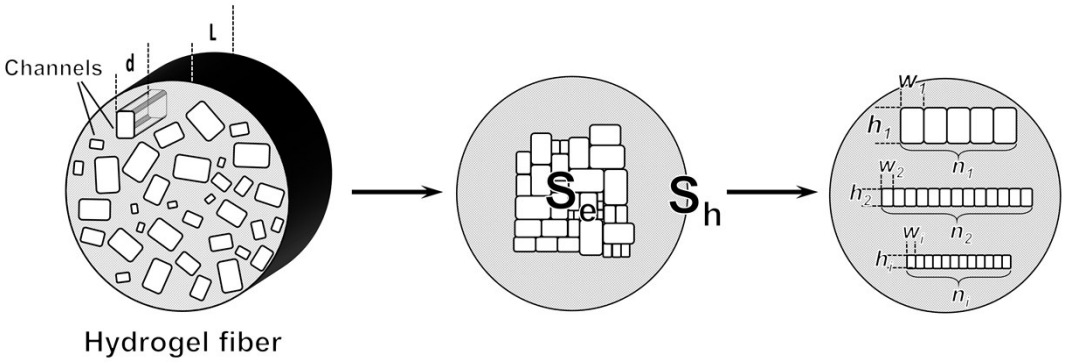

Fig. S13. From left to right: Schematic diagram of the hydrogels fibers model with ideally channels in oriented nanofibers (D = L); schematic diagram of the effective area of the channel in the model; schematic diagram of hydrogels fibers model containing channels with different size.

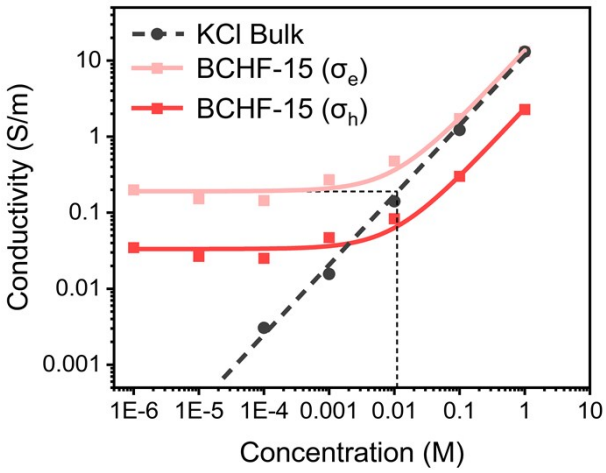

Fig. S14. The cruves of mearsured conductivity of BCHF-15 (σ_h) and the caculated effective conductivity of the channels (σ_e).

Combined with the equation S7 and the discussion above, the height of the nanochannel h_{hf} in the hydrogel fibers can be calculated by the equation S8:

$$\sigma_e = 10^{-3} z(\mu_+ + \mu_-) c N_A e + \frac{2\mu_+ \sigma_s^*}{h_{hf}} \quad (S8)$$

where the surface charge density (σ_s^*) is calculated according to equation S9:[3]

$$\sigma_s^* = \frac{\varepsilon \varepsilon_0 \zeta}{\lambda_d} \quad (S9)$$

where ε is the dielectric constant of pure water, ε_0 is the permittivity of vacuum, $\zeta[mV]$ is the mearsured zeta potential, and the Debye length λ_d in electrolyte solution can be express as equation S10:[4]

$$\frac{1}{\lambda_d} \sim \sqrt{\lambda_B I} = \sqrt{\frac{e^2}{\varepsilon \varepsilon_0 K_B T} \sum_i c_i Z_i^2} \quad (S10)$$

where e [C] is the elementary charge, K_B [J m^{-1}] is the Boltzmann constant, T is the temperature [K], λ_B [m] is Bjerrum length.

According to equation (S8–10), the Debye length is about 3 nm in a concentration of 0.01 M KCl solution, the channel height h_{hf} inside the hydrogel fiber can be calculated to be about 1.4 nm, and the surface charge density of the hydrogel fiber is calculated to be –2.97 mC m^{-2} at this time.

In fact, there are also many mesochannels and nanochannels with different size in hydrogels. According to the simplified model in Fig. S13, The effective area of the all of the channels can be expressed as equation S11:

$$S_e = \sum_i n_i w_i h_i \quad (S11)$$

where n_i, w_i [m] and h_i [m] are the number, width and height of the channels.

Then, σ_e can be expressed as equation S12:

$$\sigma_e = 10^{-3} z(\mu_+ + \mu_-) c N_A e + 2\mu_+ \sigma_s \left(\frac{\sum_i n_i w_i}{\sum_i n_i w_i h_i} \right)$$

Assuming that β_i is the ratio of the area occupied by channels with spercific size (h_i) to the total effective area, then:

$$\beta_i = \frac{n_i w_i h_i}{\sum_i n_i w_i h_i} \quad (S13)$$

And σ_e can be futher expressed as equation S14:

$$\sigma_e = 10^{-3} z(\mu_+ + \mu_-) c N_A e + 2\mu_+ \sigma_s \left(\sum_i \frac{\beta_i}{h_i} \right)$$

And σ_h can be futher expressed as according equation S7:

$$\sigma_h = \alpha [10^{-3} z(\mu_+ + \mu_-) c N_A e + 2\mu_+ \sigma_s \left(\sum_i \frac{\beta_i}{h_i} \right)] \quad (S15)$$

That means the smaller the size of the channel, the more it contributes to gain the conductivity due to the larger weight coefficient $\frac{1}{h_i}$. In other words, the more amount of channels with the smaller size, the higher the conductivity of the hydrogel fibers.

In general, for a 1 : 1 electrolyte, the value of Debye length is about 0.3–100 nm.[4, 5] The channel with a height much smaller than 0.3 nm is not considered. If the height of these channels is much greater than the Debye length even at low concentrations, the conductivity through these channels is determined by the bulk conductivity of the ionic solution ($\frac{1}{h_i}$ close to 0).

When the number of nanofibers in the hydrogel increases, the conductivity of

the hydrogel will increase due to the increased proportion of nanochannels. However, there is few nanochannel for ion transmission in CHF, and its plateau value may be due to a small part proper pore size inherent in the hydrogel fiber which can also work as nanochannels.[6, 7]

The model for change of the measured signal as a function of DA concentration

The equilibrium equations for this chemical interaction between DA and aminated anhydroglucost unit (AGU) can be written as equation S16, S17:[8]

$$(AGU-NH_2)+DA\leftrightarrow(AGU-NDA)\quad K_{DA} \tag{S16}$$

$$K_{DA}=\frac{c_{(AGU-NDA)}}{c_{(AGU-NH_2)}c_{(DA)}} \tag{S17}$$

where K_{DA} is the binding constant and c refers to the concentration, then:

$$c_{(amine)}=c_{(AGU-NH_2)}+c_{(AGU-NDA)}$$

$$c(AGU-NH_2)=\frac{1}{1+K_{DA}c_{(DA)}}c_{(amine)} \tag{S19}$$

$$c(AGU-NDA)=\frac{K_{DA}c_{(DA)}}{1+K_{DA}c_{(DA)}}c_{(amine)} \tag{S20}$$

where $c_{(amine)}$ refers to the total concentration of amine surface groups from P-BCHF.

The surface charge density (σ^*) can be expressed by the sum of the contribution of protonated free and DA-bound amine groups as equation S21,

$$\sigma^* \propto \alpha_{NH_2}c(AGU-NH_2)+\alpha_{NDA}c(AGU-NDA) \tag{S21}$$

where α_{NH_2} is the degree of the unmodified amine groups that can be protonated, α_{NDA} is the degree of DA-modified sites that can be protonated, and it is expected that $\alpha_{NH_2}>\alpha_{NDA}$ according to the chemical structures.[9]

According to equation S19 and S20, $\sigma^*_{(c)}$ at a certain concentration of DA can also be express as equation S22:

$$\sigma^*_{(c)}\propto\frac{\alpha_{NH_2}+\alpha_{NDA}K_{DA}c_{(DA)}}{1+K_{DA}c_{(DA)}}c_{(amine)} \tag{S22}$$

When there is no DA solution, the surface charge density corresponding to the protonated amine group (σ^*_0) can be expressed as equation S23 by simplifying

equation S22:

$$\sigma_0^* \propto \alpha_{NH_2} c_{(amine)} \quad (S23)$$

And the surface charge density under conditions of sufficient DA (σ_{max}^*) can also be expressed as equation S24:

$$\sigma_{max}^* \propto \alpha_{NDA} c_{(amine)} \quad (S24)$$

Then the change of surface charge density can be expressed as equation S25:

$$\frac{\sigma_0^* - \sigma_{(c)}^*}{\sigma_0^* - \sigma_{max}^*} = \frac{K_{DA} c_{(DA)}}{1 + K_{DA} c_{(DA)}} = \theta \quad (S25)$$

where θ can be seen as the fractional coverage of the molecule on the surface, K_{DA} is the combine constant, c is the concentration of target molecules. In fact, this formula is similar to the Langmuir adsorption equation, which is also used in the quantitative analysis of nanochannel sensors.

According to S3, there is a linear relationship between σ^* and G. And obviously, there is a linear relationship between between G and I, so the equation S25 can be express as equation (S26):

$$\frac{I_0 - I_{(c)}}{I_0 - I_{max}} = \frac{K_{DA} c_{(DA)}}{1 + K_{DA} c_{(DA)}} \quad (S26)$$

where I_0 is the current obtained in the absence of DA, $I_{(c)}$ is the current observed at specific DA concentration, and I_{max} is the current for an DA concentration of 10 μM. In fact, this formula is similar to the Langmuir adsorption equation, which is also used in the quantitative analysis of nanochannel sensors. And the right half of equation S26 is always called fractional coverage (θ) in the Langmuir adsorption equation.

The curve obtained by fitting conforms to the law of equation S26 (R=0.81). The equation S26 is derived from S3 instead of modified equation S15 for the convenience of calculation. That means the deviation may be due to the presence of mesopores in the hydrogel fibers, and the conductivity of which is not dominated by surface charges.

Table 1 Water content and diameter of BCHFs with different urea content.

	Urea content	Spinning speed	Water content (%)	Diameter* (μm)
BCHF-10	10 wt%	2.4 m/min (300 μL/min)	90.7 ± 1.3	330.4
BCHF-15	**15** wt**%**	**2.4 m/min (300 μL/min)**	**87.0 ± 0.3**	**326.2**
BCHF-20	20 wt%	2.4 m/min (300 μL/min)	83.3 ± 3.8	267.7
BCHF-25	25 wt%	2.4 m/min (300 μL/min)	85.7 ± 3.0	271.2
CHF	15 wt%	2.4 m/min (300 μL/min)	84.6 ± 1.9	312.6

*The average diameter was measured for more than ten hydrogel fibers under an optical microscope.

Table 2 Mechanical properties of BCHFs with different urea content

	Urea content	Spinning speed	Modulus (MPa)	Tensile Strength (MPa)
BCHF-10	10 wt%	2.4 m/min (300 μL/min)	1.13 ± 0.23	0.75 ± 0.11
BCHF-15	**15 wt%**	**2.4 m/min (300 μL/min)**	**3.39 ± 0.09**	**3.74 ± 0.37**
BCHF-20	20 wt%	2.4 m/min (300 μL/min)	2.16 ± 0.18	2.29 ± 0.10
BCHF-25	25 wt%	2.4 m/min (300 μL/min)	1.31 ± 0.05	0.99 ± 0.13
CHF-15	15 wt%	2.4 m/min (300 μL/min)	1.81 ± 0.33	0.99 ± 0.23

Table 3 Mechanical properties of BCHF-15 with different spinning speeds.

	Urea content	Spinning speed	Modulus (MPa)	Tensile Strength (MPa)
BCHF-15-0.8	15 wt%	0.8 m/min (100 μL/min)	2.07 ± 0.46	1.67 ± 0.37
BCHF-15-2.4	**15 wt%**	**2.4 m/min (300 μL/min)**	**3.39 ± 0.09**	**3.74 ± 0.37**
BCHF-15-7.2	15 wt%	7.2 m/min (900 μL/min)	**3.52 ± 0.35**	3.41 ± 0.74
BCHF-15-24	15 wt%	24 m/min (3000 μL/min)	2.55 ± 0.48	2.12 ± 0.32

Table 4 Mechanical properties of BCHF-20 with different spinning speed.

	Urea content	Spinning speed	Modulus （MPa）	Tensile Strength （MPa）
BCHF-20-0.8	20 wt%	0.8 m/min (100 μL/min)	1.76 ± 0.46	1.53 ± 0.22
BCHF-20-2.4	**20 wt%**	**2.4 m/min (300 μL/min)**	**2.16 ± 0.18**	**2.29 ± 0.10**
BCHF-20-7.2	20 wt%	7.2 m/min (900 μL/min)	**2.47 ± 0.45**	1.67 ± 0.51
BCHF-20-24	20 wt%	24 m/min (3000 μL/min)	**2.46 ± 0.61**	1.58 ± 0.29

References

1. Y.-C. Yao, A. Taqieddin, M. A. Alibakhshi, M. Wanunu, N. R. Aluru and A. Noy, *ACS Nano*, 2019, **13**, 12851-12859.
2. C. Yang and Z. Suo, *Nat. Rev. Mater.*, 2018, **3**, 125-142.
3. H.-R. Lee, C.-C. Kim and J.-Y. Sun, *Adv. Mater.*, 2018, **30**, 1704403.
4. J. P. Thiruraman, P. Masih Das and M. Drndić, *ACS Nano*, 2020, **14**, 3736-3746.
5. M. Napoli, J. C. T. Eijkel and S. Pennathur, *Lab Chip*, 2010, **10**, 957-985.
6. B. Bao, J. Hao, X. Bian, X. Zhu, K. Xiao, J. Liao, J. Zhou, Y. Zhou and L. Jiang, *Adv. Mater.*, 2017, **29**, 1702926.
7. W. Chen, Q. Wang, J. Chen, Q. Zhang, X. Zhao, Y. Qian, C. Zhu, L. Yang, Y. Zhao, X.-Y. Kong, B. Lu, L. Jiang and L. Wen, *Nano Lett.*, 2020, **20**, 5705-5713.
8. G. Laucirica, W. A. Marmisollé and O. Azzaroni, *Phys. Chem. Chem. Phys.*, 2017, **19**, 8612-8620.
9. G. Laucirica, Y. Toum Terrones, V. M. Cayón, M. L. Cortez, M. E. Toimil-Molares, C. Trautmann, W. A. Marmisollé and O. Azzaroni, *Nanoscale*, 2020, **12**, 18390-18399.